

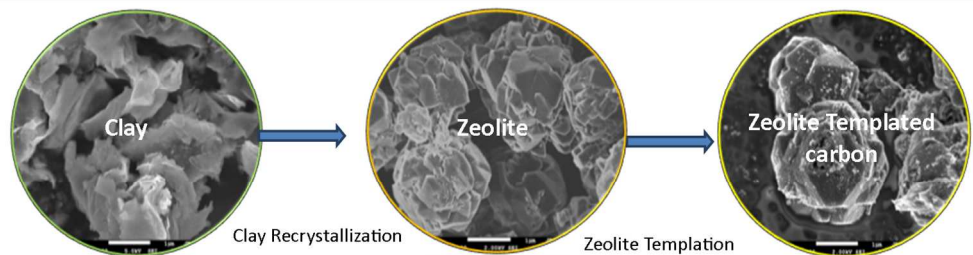


Synthesis of templated carbons starting from clay and clay-derived zeolites for hydrogen storage applications

Journal:	<i>International Journal of Energy Research</i>
Manuscript ID:	ER-14-4650.R1
Wiley - Manuscript type:	Research Article
Date Submitted by the Author:	n/a
Complete List of Authors:	<p>Musyoka, Nicholas; HySA Infrastructure Centre of Competence, Council for Scientific and Industrial Research (CSIR), Materials Science and Manufacturing</p> <p>Ren, Jianwei; HySA Infrastructure Centre of Competence, Council for Scientific and Industrial Research (CSIR), Materials Science and Manufacturing</p> <p>Langmi, Henrietta; HySA Infrastructure Centre of Competence, Council for Scientific and Industrial Research (CSIR), Materials Science and Manufacturing</p> <p>Rogers, David; HySA Infrastructure Centre of Competence, Council for Scientific and Industrial Research (CSIR), Materials Science and Manufacturing</p> <p>North, Brian; HySA Infrastructure Centre of Competence, Council for Scientific and Industrial Research (CSIR), Materials Science and Manufacturing</p> <p>Mathe, Mkhulu; HySA Infrastructure Centre of Competence, Council for Scientific and Industrial Research (CSIR), Materials Science and Manufacturing</p> <p>Bessarabov, Dmitri; HySA Infrastructure Centre of Competence, North West University, Faculty of Engineering</p>
Keywords:	Clay, Templated carbon, Recrystallization, Zeolites, Hydrogen storage, chemical vapour deposition

SCHOLARONE™
Manuscripts

1
2
3
4
5
6
7
8
9
10
11
12
13
14
15
16
17
18
19
20
21
22
23
24
25
26
27
28
29
30
31
32
33
34
35
36
37
38
39
40
41
42
43
44
45
46
47
48
49
50
51
52
53
54
55
56
57
58
59
60



281x77mm (150 x 150 DPI)

For Peer Review

Synthesis of templated carbons starting from clay and clay-derived zeolites for hydrogen storage applications

N. M. Musyoka^{1*}, J. Ren¹, H. W. Langmi¹, D. E. C. Rogers¹, B. C. North¹, M. Mathe¹ and D. Bessarabov²

¹HySA Infrastructure Centre of Competence, Materials Science and Manufacturing, Council for Scientific and Industrial Research (CSIR), P.O. Box 395, Pretoria 0001, South Africa. ²HySA Infrastructure Centre of Competence, North West University, P. Bag X6001, Potchefstroom 2520, South Africa. *Corresponding author: Tel.: +27-12-841-4806, Fax: +27-12-841-2135, E-mail address: NMusyoka@csir.co.za

SUMMARY

Clay and its recrystallized zeolitic derivatives were used in this study as templating agents for carbon nanostructured materials. The conventional nanocasting process that involves impregnation with furfural alcohol and subsequent chemical vapour deposition was followed. Several techniques such as X-ray diffraction (XRD), scanning electron microscopy (SEM), thermo-gravimetric analysis (TGA) and surface area analysis were used to characterize the parent templating materials including the resulting nanocasted carbons. The study demonstrated that there is greater potential for the use of value-added clays rather than their pristine form, and hence presents a cost effective alternative for producing carbonaceous materials with more attractive properties for hydrogen storage applications.

KEYWORDS

Clay, templated carbon, hydrogen storage, recrystallization, zeolites, chemical vapour deposition

1. Introduction

Hydrogen storage in carbonaceous materials is receiving significant attention in the scientific community due to their high hydrogen uptakes (Nishihara and Kyotani, 2012). Of the many available porous carbonaceous options, templated carbons have shown a greater promise and are being studied extensively (Xia et al., 2013). The process of nanocasting enables predetermined control of pore structure properties of the resulting carbon with improved ease. These porous carbon-based materials are also known to possess high surface areas, large pore volumes, low densities, high thermal and chemical stabilities, and are also easy to scale up (Chen et al., 2007; Alam and Mokaya, 2010; Yang et al., 2012). Among the many reported nanocasted carbons (Nishihara and Kyotani, 2012), zeolite templated carbons have stood out as the most promising carbon-based materials reported to date since they possess superior hydrogen storage capacities. Even though an earlier study by Meyers et al. (2001) had pointed out the possibility of preparing templated carbons starting from commercially available montmorillonite clay, subsequent research work has mainly focused on zeolites produced from conventional chemicals. To the best of the authors' knowledge, this is the first instance in the literature that reports on the use of zeolites derived from clays as templating agents for nanocasted carbons.

In a recent review paper by Nishihara and Kyotani (2012), it was suggested that the application of low-cost templating materials would play a significant role in lowering the potentially high production cost of templated carbons. Therefore this study not only uses the value added clay derivatives as carbon templates but also compares the effect of using clay materials sourced from different locations. The study further examines the hydrogen storage capacities of these materials. With the understanding that zeolite templated carbons offer superior properties compared to clay-templated carbons, there is no doubt that beneficiation of clays would offer a cost effective alternative to produce carbonaceous materials with more attractive properties especially for energy storage applications. Since the production of zeolite templated carbons is now relatively well established (Xia et al., 2010; Konwar and De, 2014), the conventional templating process that involves three steps; the introduction of suitable carbon precursors into the pores of an inorganic hard template, followed by carbonization at high temperature under inert conditions, and finally, removal of the inorganic template to generate porous carbon was followed in this study.

2. Experimental

2.1 Synthesis materials

Natural sodium montmorillonite clay (NC), with a trade name of cloisite Na⁺ was obtained from Southern Clay Products Inc., Texas, USA (now a part of BYK Additives) whereas bentonite clay (SBC) was obtained from Ecce Holdings Mine Company in South Africa. Three clay derived zeolite X samples were prepared according to the experimental procedure reported by Musyoka et al. (2014). These samples were code labelled as follows; CNC for zeolite from clear (filtered) extract of cloisite clay, SNC for zeolite from unfiltered cloisite clay extract and SBC for zeolite from unfiltered South African bentonite clay extract. Furfuryl alcohol (Sigma Aldrich, C₅H₆O₂, 98%) and Ethylene gas were used as the carbon precursors. Ethanol (Merck, 99.5%) was used as solvent. Hydrofluoric (Merck, 40%) and hydrochloric acids (Ace, 32%) were used to remove the inorganic template from the resulting carbon.

2.2 Preparation of templated carbons

Clay and clay-derived samples were dried in an oven at 250 °C for 12 h prior to liquid impregnation using furfural alcohol (FA). Thereafter the FA impregnated samples were washed with a small quantity of ethanol to remove excess furfural alcohol. The resulting clay or clay-derived/FA composites were independently placed in alumina combustion sample boats and transferred into a tube furnace where they were polymerized at 80 °C for 24 h and subsequently for another 8 h at 150 °C. This polymerization step was conducted under the flow of argon gas at a flow rate of 100 ml/min. The tube furnace temperature was later increased to 700 °C at a heating rate of 5 °C/min and held there for 3 h, still under argon flow, to allow carbonization of the polymerized furfural alcohol. Thereafter, an ethylene/argon gas mixture (10:90) was flushed through the tube furnace, still at 700 °C, for 3 hours. Thereafter, only argon gas was allowed to flow and the temperature was raised to 900 °C for an additional 3 h to allow carbonization of the chemical vapour deposited carbon. The resulting materials were treated with hydrofluoric acid for 3 h at room temperature and later refluxed with hydrochloric acid for 3 h at 60 °C in order to demineralize the clay and zeolitic template. The obtained material was further washed with de-ionized water and dried overnight at 120 °C. The resulting samples were designated as follows; TNC for templated carbon from cloisite clay, TCNC for zeolite templated carbon from clear extract of cloisite clay, TSNC for zeolite templated carbon from unfiltered cloisite clay extract and TSBC for zeolite templated carbon from unfiltered South African bentonite clay extract.

2.2 Characterization

Powder X-ray diffraction (PXRD) analysis was conducted using a PANalytical X'Pert Pro powder diffractometer, fitted with a Pixcel detector and with Cu-K α radiation (0.154 nm). The data was collected within the range of $2\theta = 4 - 60^\circ$. Morphological analysis was performed using a scanning electron microscope (Jeol-JSM 7500F). Prior to analysis, samples were transferred onto an aluminium stud laced with a carbon tape and carbon coated to avoid charging during analysis. Thermal stability analysis was performed using a thermogravimetric analysis (TGA) instrument (Mettler, Toledo, TGA/SDTA 851^e). In this case, about 10 mg of the sample was loaded in an alumina crucible and heated to 1000 °C at a rate of 10 K · min⁻¹ with an air gas flow of 10 mL · min⁻¹. This analysis was used to check and confirm the degree of the nanocasting procedure. Surface area and porosity measurements were carried out using an ASAP 2020 HD analyzer (Micromeritics) using nitrogen gas. BET surface areas were obtained from the linear region of the N₂ isotherms following the criterion reported in the literature (Rouquerol et al., 2007). Hydrogen adsorption isotherms, at 77 K and up to 1 bar, were also measured on the ASAP 2020 instrument. All gas sorption isotherms were obtained using ultra-high purity grade (99.999%) gas. Before analysis, the samples were outgassed for 480 min at 350 °C in the degassing port with further degassing at 300 °C for 180 min in the analytical port.

3. Results and discussion

To evaluate the transformation that took place during the templation process, X-ray diffraction analyses for the starting cloisite clay material, its zeolitic derivatives as well as their respective templated carbonaceous derivatives were carried out and the results are shown in Fig. 1. The XRD patterns of the as-received cloisite clay (Fig. 1a) confirmed that it was indeed a montmorillonite type. Clay materials are widely known to have a layered crystalline structure and are subject to shrinking and swelling when water is absorbed or removed from the layers. Musyoka and co-workers (2014) reported that the type and structure of the resulting zeolitic phase depends on the mineralogical and chemical composition of the synthesis feedstock as well as the synthesis conditions. In this case, the choice of the type of zeolite template would be expected to influence the quality and properties of the templated carbon as well as its hydrogen uptake. The XRD patterns of the clay-derived zeolite obtained from the filtered (clear) cloisite clay extract (Fig. 1b) showed that it was mainly comprised of a mixture of zeolite P and X phases. The formation of the mixed phase could be advantageous since the two

1
2
3 types of zeolites are known to have different pore size distributions which would create a
4 hierarchical system that might facilitate access of adsorbate molecules (diffusion) to the
5 smaller pores of zeolite P via the relatively larger pores of zeolite X. Fig. 1c shows that zeolite
6 X was the main zeolitic phase obtained from the unfiltered cloisite clay extract. It was of
7 interest to investigate the effect of using these different zeolite templates to produce
8 carbonaceous materials since differences in their morphological features would be expected to
9 play a key role in determining their hydrogen storage properties.
10
11
12
13
14
15

16 The XRD pattern of the templated carbon samples from cloisite clay (Fig. 1a) exhibited a
17 peak at around $2\theta = 7^\circ$, which indicates regular ordering, with periodicity of about 1.2 nm in
18 the carbon structure, as also suggested by other researchers (Meyers et al. 2001). In the same
19 manner, XRD patterns of the templated carbons from the clay-derived zeolites (Fig. 1a and b)
20 also confirmed the presence of zeolite-like pore ordering (i.e. $\{111\}$ planes of the ordered
21 framework) due to the presence the peak around $2\theta = 6-7^\circ$, as also indicated by Chen et al.
22 (2007). All the templated carbon materials from both clay and clay-derived zeolites exhibited
23 a broad peak of relatively lower intensity at about $2\theta = 25^\circ$ which could indicate the
24 presence of graphene layers, nano graphene networks or graphene stacking as reported by
25 Amandi et al. (2008), Itoi et al. (2014) and Yang et al. (2012). The appearance of a low
26 intensity peak at around $2\theta = 17^\circ$ in the templated carbons derived from cloisite clay as well
27 as from the zeolitic material from the clear extract of cloisite clay could be associated with
28 the presence of inter-grown carbon nanotubes (CNTs) which could also be seen in the SEM
29 images (Fig. 2a and b). Morphological analysis of cloisite clay (Fig. 2a) showed that the clay
30 contained uneven platelets with poorly defined ragged-edged flakes. Whereas the
31 morphology of the zeolitic materials obtained from clear extract of clay (Fig. 2b) had a
32 mixture of both cactus-like and octahedral pyramidal shapes that corresponded to the
33 expected morphologies of both zeolite P and X. The sharp-edged crystals confirmed that the
34 sample was well crystallized. The zeolite from the unfiltered cloisite clay extract (Fig. 2c)
35 had scruffy sub-rounded particles that were not easily related to the zeolite X identified in
36 Fig. 1c. The failure to get the expected well-defined octahedral pyramidal particles suggests
37 that the zeolite was not fully crystalline as noted from its XRD pattern. Morphological
38 analyses of all the three templated carbons (Fig 2a, b and c) confirmed that the obtained
39 products were a replica of their respective starting templating material. In the case of the
40 templated carbon from cloisite clay and its zeolitic derivative from the filtered extract (Fig.
41 2a and b), there was evidence that some carbon nanotubes (CNTs) were also obtained and
42
43
44
45
46
47
48
49
50
51
52
53
54
55
56
57
58
59
60

1
2
3 correlated well with the XRD peak that had been observed at around $2\theta = 17^\circ$. The presence
4 of transition metals (e.g. Fe, Ni, Co, Mo, etc) in the as-received clay material and traces in the
5 synthesized zeolite are subject for further investigation on their possible role as a catalyst for
6 the growth of CNTs.
7
8

9
10 From the TGA analysis of the raw cloisite clay (Fig. 3a - NC), it can be noted that a weight
11 loss of $\sim 10\%$, which corresponded to thermal desorption of adsorbed water, occurred
12 between 100 - 150 °C. Further weight loss was noted to occur between 600 and 680 °C and
13 could be related to the destruction of hydroxyl bonds that are formed when certain cations,
14 present within the clay material, polarize water molecules. During this process further
15 expulsion of more water from the intra-crystalline cavities of the clay occurs. There was no
16 further significant weight loss observed between 680 and 1000 °C. The TGA plots of zeolites
17 synthesized from the filtered (Fig. 3b - CNC) and unfiltered (Fig. 3c - SNC) extract of cloisite
18 clay both showed that $\sim 20\%$ weight loss occurred mainly within the initial 200 °C of heating
19 and thereafter the weight remained almost constant up to 1000 °C. The weight loss occurring
20 below 200 °C can be ascribed to the loss of adsorbed and hydrated water from the zeolitic
21 matrix. No evidence of dehydroxylation was observed as there was no weight loss in the
22 range of 300-450 °C. The main weight loss in all the templated carbons was observed in the
23 temperature range of 450–650 °C and thereafter the weight remained almost constant up to
24 1000 °C. This thermogravimetric behavior corresponds to the carbon burning out in air and
25 hence shows that successful templation process had taken place since the weight loss was up
26 to $\sim 98\%$ within the temperature range of 600–1000 °C. This range was also found to be
27 similar to that observed by Masika and Mokaya (2013). Complimenting EDX analysis (not
28 reported here) also confirmed the expectation that the templated materials were mainly
29 composed of carbon.
30
31
32
33
34
35
36
37
38
39
40
41
42
43
44

45
46 The N_2 -sorption isotherms of the cloisite clay, as well as their respective clay-derived and
47 zeolite-derived templated carbons were found to be of type IV due to the irreversible pore
48 condensation in the N_2 isotherms shown in Fig. 4. The recrystallized derivatives were found
49 to be Type I with the limiting uptake being due to the accessible micropore volume rather
50 than the internal surface area (Sing et al., 1985). A summary of BET surface areas is
51 presented in Table 1. The surface area of cloisite clay was noted to be considerably lower
52 when compared to its zeolitic derivatives. This observation can be explained by their
53 respective mineralogical, morphological and structural differences as shown in Figs. 1, 2 and
54
55
56
57
58
59
60

1
2
3 3. Raw clays are known to possess porosity mainly due to their inter-lamellar and inter-
4 particle spaces whereas during the zeolitization process, structural readjustments and re-
5 organization that leads to creation of a well-defined network of pores within the zeolite
6 crystals occur at a nanometric and/or micrometric scale, depending on the type of zeolite
7 formed. Other contributions to porosity could also come from the inter-particle porosity,
8 which is often at a mesopore range (2 and 50 nm). In a type IV and type 1 isotherms, the
9 steep initial region of the adsorption isotherm is due to the very strong adsorption in the
10 micropores (Lowell et al., 2006). This characteristic behaviour was found to be missing from
11 the cloisite clay isotherm meaning that it does not possess micropores accessible to N₂, unlike
12 its zeolitic derivatives. The hysteresis loop in the N₂-sorption isotherms indicates irreversible
13 condensation in the meso and macropores. The hysteresis of the clay sample was found to be
14 more pronounced than those of the other templating materials meaning that it had more meso
15 porosity. As shown in Table 1, the BET surface areas of the templated carbons obtained from
16 both the raw cloisite as well as from its zeolitic derivatives were found to be significantly
17 higher than those of the respective templating parent materials. This increase in BET surface
18 area can be ascribed to the well-ordered microporosity occurring after removal of the
19 template. Notably, it is worth mentioning that the surface areas reported herein were also
20 found to be higher than those reported by Meyer et al. (2001), and this could be attributed to
21 the advancements in the templation process since Meyer's studies were conducted.
22 Information from the BET surface area of a microporous material is sometimes used to
23 generate a rough estimate for the hydrogen storage capacity. Some recent studies have
24 reported that there exists a nearly linear relationship between the specific surface area of
25 porous material and its hydrogen storage capacity (Xia et al., 2013).
26
27
28
29
30
31
32
33
34
35
36
37
38
39
40
41
42

43 Similarly to the trend observed in the BET surface areas in Table 1, the templated carbons
44 obtained from zeolites were noted to have higher hydrogen uptakes than those obtained from
45 the as-received clay. Even though some other studies have analyzed the hydrogen uptake at
46 20 bar (Xia et al., 2013), measurements at 1 bar provides a good basis for understanding the
47 quality of the sample. The use of zeolites as templating material is often attractive due to their
48 versatility and presence of well-defined, three-dimensional, pore structures that enables
49 intentional control of pore properties as well as the morphology of the resulting porous
50 carbon. A recent review by Nishihara and Kyotani (2012) pointed out that the most important
51 property for hydrogen storage in the porous materials at 77 K lies with the material's ability
52 to possess micropores rather than macro and mesopores. This behavior is also confirmed in
53
54
55
56
57
58
59
60

1
2
3 this study (see Table 1) whereby the templated carbons were found to possess higher
4 hydrogen storage capacities compared to their respective parent templating materials. Even
5 though the specific surface areas of porous carbon materials cannot be increased infinitely
6 (Xia et al., 2013), porosity at the nano and micro levels is known to immensely contribute to
7 the enhancement of the performance of porous carbon in hydrogen storage applications
8 (Nishihara and Kyotani, 2012). The storage of hydrogen in porous materials via the
9 physisorption process is mainly driven by the presence of weak interaction forces (van der
10 Waals) that exist between the hydrogen molecules and the adsorbent surface (Chen et al.,
11 2007; Wang and Yang, 2012). Previous studies have reported that the presence of a large
12 number of ultramicropores leads to a stronger interaction between carbon and hydrogen and
13 hence a higher isosteric heat of adsorption when compared to samples with fewer or no
14 ultramicropores (Alam and Mokaya, 2010).
15
16
17
18
19
20
21
22
23

24 Even though physisorption of hydrogen in microporous materials has normally been reported
25 for uptake mainly at cryogenic temperature (Xia et al., 2013), various strategies for boosting
26 hydrogen uptake in porous materials such as by doping with heteroatoms (e.g. nitrogen and
27 sulphur) and also by spillover effect especially on the surface of metal particles (e.g. Pt) have
28 been reported to enhance hydrogen storage capacities at room temperature (Nishihara and
29 Kyotani, 2012; Juárez et al., 2014). As would be expected, the relatively higher surface area
30 of the zeolitic sample that was synthesized from the filtered extract of cloisite clay (Fig. 4b -
31 CNC) had a higher hydrogen storage capacity when compared to that obtained from the
32 unfiltered clay extract (Fig. 4C – SNC). This observation further reinforces the explanation
33 about the differences in pore sizes and pore structures that exist between zeolite P and X. The
34 low hydrogen uptake especially in the templated carbons from raw cloisite clay (Fig. 4a -
35 TNC) as well as its zeolitic derivative from the filtered extract (Fig. 4c –TCNC) can also be
36 explained by the results shown in Figs. 1 and 2, in which case carbon nanotubes were
37 observed to have formed during the templation process. Even though there was earlier
38 excitement about the tremendous potential for storing hydrogen in carbon nanotubes (He et
39 al., 2013), later studies disapproved those claims due to inaccuracies in hydrogen uptake
40 measurements as well as the limited understanding of the mechanisms of hydrogen storage
41 (Xia et al., 2013). The enhancement of hydrogen storage in CNTs and other porous
42 carbonaceous materials, occurring after metal loading, has been reported to occur as a result
43 of the spillover effect (Bhowmick et al., 2011). Hydrogen spillover is often defined as the
44 dissociative chemisorption of hydrogen in the presence of metal nanoparticles which in turn
45
46
47
48
49
50
51
52
53
54
55
56
57
58
59
60

1
2
3 leads to subsequent migration of hydrogen atoms onto the neighbouring surfaces of a receptor
4 material (Wang and Yang, 2012).
5
6

7
8 The South African bentonite-derived zeolite templated carbon was also prepared and
9 investigated in order to compare the effect of using zeolites synthesized from different sources
10 of clay. Fig. 5 shows the XRD (5a), SEM (5b), N₂-sorption isotherm (5c) and the hydrogen
11 storage capacity (5d) of the South African bentonite-derived zeolite templated carbon. From
12 the XRD patterns, it can be noted that whilst the same synthesis conditions were followed, a
13 much better crystalline single phase zeolite X was obtained and its templated carbon did not
14 have significant contamination of carbon nanotubes like had been observed when cloisite clay
15 was used (Fig. 1a). The respective SEM images also show that the nanocasting process was
16 successful since the morphology of the templated carbon was similar to that of its parent zeolite
17 X. The surface area and hydrogen storage capacity of the South African bentonite-based zeolite
18 templated carbon was also found to be relatively higher than its cloisite clay-based zeolite
19 templated carbon counterpart. These findings serve to highlight the conclusion that different
20 clays and their templated carbons, as well as their zeolitic and template carbon derivatives have
21 different properties, and independent optimization conditions for enhanced hydrogen storage
22 should be investigated. These differences can primarily be attributed to the differences in
23 chemical, mineralogical and structural composition of the parent clays. If these factors are
24 investigated prior to their use and modifications, there may be potential to obtain almost the
25 same hydrogen uptake properties as those of commercially available templating materials.
26
27
28
29
30
31
32
33
34
35
36
37
38
39

40 **4. Conclusion**

41 In summary, the present study has evaluated the potential for the use of less expensive clays
42 and their zeolitic derivatives as template materials during the synthesis of nanostructured
43 carbons for hydrogen storage applications. The clay-derived zeolite templated carbons were
44 obtained with a BET surface area in the range of 214-569 m²/g and a hydrogen uptake of 0.3
45 - 0.7 wt%, depending on the type and source of the clay-derivative. The mimicking of the
46 porosity of zeolitic material, which for this case is at nano to micropore level led to a higher
47 hydrogen storage capacity in the zeolite templated carbon when compared to the clay
48 templated carbon. The failure to obtain higher surface areas and hydrogen storage, as would
49 have been expected, was ascribed to the formation of carbon nanotubes during the chemical
50 vapour deposition step. The study further demonstrates that there is greater potential for the
51 use of value-added clays (zeolitic derivatives) rather than their pristine form, and hence
52
53
54
55
56
57
58
59
60

1
2
3 presents a cost effective alternative for producing carbonaceous materials with more
4 attractive properties for hydrogen storage applications. In the next phase of our study,
5 modifications such as ion exchange prior to the templation process as well as
6 functionalization studies will be conducted to further enhance the hydrogen uptake capacities.
7
8
9

10 11 **Acknowledgements**

12 The authors of this paper would like to acknowledge the financial support from the South
13 African Department of Science and Technology (DST) for the HySA programme.
14
15
16

17 18 **References**

- 19 1. Nishihara, H., Kyotani, T. Templated Nanocarbons for Energy Storage. *Adv. Mater.*
20 2012; 24: 4473–4498.
21
22
- 23 2. Yang, J. S., Jung, H., Kim, T., Park, C. R. Recent advances in hydrogen storage
24 technologies based on nanoporous carbon materials. *Prog. Nat. Sci. Mater. Int.* 2012; 22:
25 631–638.
26
27
- 28 3. Alam, N., Mokaya, R. Evolution of optimal porosity for improved hydrogen storage in
29 templated zeolite-like carbons. *Energy Environ. Sci.*, 2010; 3: 1773-1781.
30
31
- 32 4. Xia, Y., Yang, Z., Zhu, Y. Porous carbon-based materials for hydrogen storage:
33 advancement and challenge. *J. Mater. Chem. A*, 2013; 1: 9365-9381.
34
35
- 36 5. Bhowmick, R., Rajasekaran, S., Friebel, D., Beasley, C., Jiao, L., Ogasawara, H., Dai, H.,
37 Clemens, B., Nilsson, A. Hydrogen spillover in Pt-single-walled carbon nanotube
38 composite: Formation of stable C-H bonds. *J. Am. Chem. Soc.* 2011; 133: 5580-5586.
39
40
- 41 6. Armandi, M., Bonelli, B., Arean, C. O., Garrone, E. Role of microporosity in hydrogen
42 adsorption on templated nanoporous carbons. *Micropor. Mesopor. Mater.*, 2008; 112:
43 411–418.
44
45
- 46 7. Wang, L., Yang, R. T. Molecular hydrogen and spillover hydrogen storage on high
47 surface area carbon sorbents. *Carbon.* 2012; 50: 3134-3140.
48
49
50
51
52
53
54
55
56
57
58
59
60

- 1
2
3
4
5 8. Lowell, S., Shields, J. E., Thomas, M. A. Characterization of porous solids and powders:
6 surface area, pore size and density, Springer (2006). ISBN:1402023022
7
8
9
- 10
11 9. Chen, L., Singh, R. K., Webley. P. Synthesis, characterization and hydrogen storage
12 properties of microporous carbons templated by cation exchanged forms of zeolite Y with
13 propylene and butylene as carbon precursors. *Micropor. Mesopor. Mater.*, 2007; 102:
14 159–170.
15
16
- 17
18
19 10. Meyers, C. J. Shah, S. D., Patel, S. C., Sneeringer, R. M., Bessel, C. A., Dollahon, N R.,
20 Leising, R. A., Takeuchi E. S. Templated Synthesis of Carbon Materials from Zeolites
21 (Y, Beta, and ZSM-5) and a Montmorillonite Clay (K10): Physical and Electrochemical
22 Characterization. *J. Phys. Chem. B* 2001; 105: 2143 -2152.
23
24
- 25
26
27 11. Rouquerol J, Llewellyn P, Rouquerol F. Is the BET equation applicable to microporous
28 adsorbents? *Stud Surf Sci Catal* 2007; 160: 49–56.
29
30
- 31
32 12. Xia, Y. D., Yang, Z. X. and Mokaya, R. CVD nanocasting routes to zeolite-templated
33 carbons for hydrogen storage. *Chem. Vap. Deposition.* 2010; 16: 322-328.
34
35
- 36
37 13. Musyoka, N. M., Missengue, R., Kuisakana, M., Petrik, L. Conversion of South African
38 clays into high quality zeolites. *Appl. Clay Sci.* 2014; 97–98: 182–186.
39
40
- 41
42 14. Masika, E., Mokaya, R. Preparation of ultrahigh surface area porous carbons templated
43 using zeolite 13X for enhanced hydrogen storage. *Prog. Nat. Sci. Mater. Int.* 2013; 23:
44 308 – 316.
45
46
- 47
48 15. Itoi, H., Nishihara, H., Ishii, T., Nueangnoraj, K., Berenguer-Betrián, R., Kyotani, T.
49 Large Pseudocapacitance in Quinone-Functionalized Zeolite-Templated Carbon. *Bull.*
50 *Chem. Soc. Jpn.* 2014; 87: 250-257.
51
52
- 53
54 16. Sing, K. S. W., Everett, D. H., Haul, R. A. W., Moscou, L., Pierotti, R. A., Rouquerol, J.,
55 Siemieniewska, T. Reporting physisorption data for gas/solid systems with special
56 reference to the determination of surface area and porosity (Recommendations 1984).
57 *Pure Appl. Chem.*, 1985; 57: 603-619.
58
59
60

- 1
2
3
4 17. Konwar, R. J., De, M. Development of templated carbon by carbonisation of sucrose-
5 zeolite composite for hydrogen storage. *Int. J. Energy Res.* 2014; doi: 10.1002/er.3232;
6
7
8
9 18. He, Z., Wang, S., Wang, X., Iqbal, Z. Hydrogen storage in hierarchical nanoporous
10 silicon – carbon nanotube architectures. *Int. J. Energy Res.* 2013; 37: 754 –760.
11
12
13
14 19. Juárez, J. M., Costa, M. B., Anunziata, O. A. Synthesis and characterization of Pt-CMK-3
15 hybrid nanocomposite for hydrogen storage. *Int. J. Energy Res.* 2014; doi:
16 10.1002/er.3229.
17
18
19
20
21
22
23
24
25
26
27
28
29
30
31
32
33
34
35
36
37
38
39
40
41
42
43
44
45
46
47
48
49
50
51
52
53
54
55
56
57
58
59
60

For Peer Review

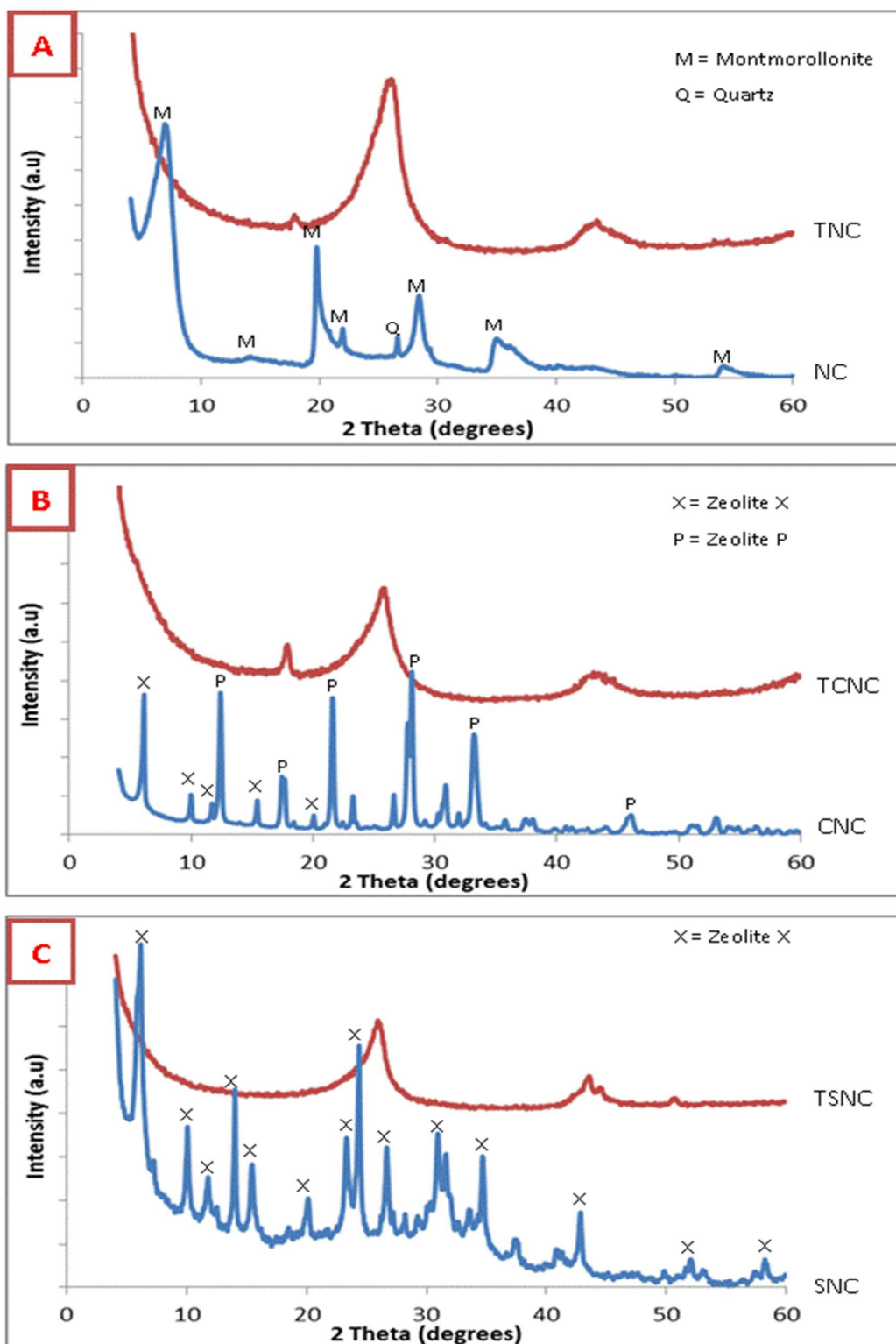


Figure 1: XRD patterns of A) Cloisite clay (NC), and its templated carbon (TNC); B) Zeolite synthesized from clear extract of cloisite clay (CNC), and its template carbon (TCNC); and C) Zeolite synthesized from slurry-form of cloisite clay (SNC), and its template carbon (TSNC).

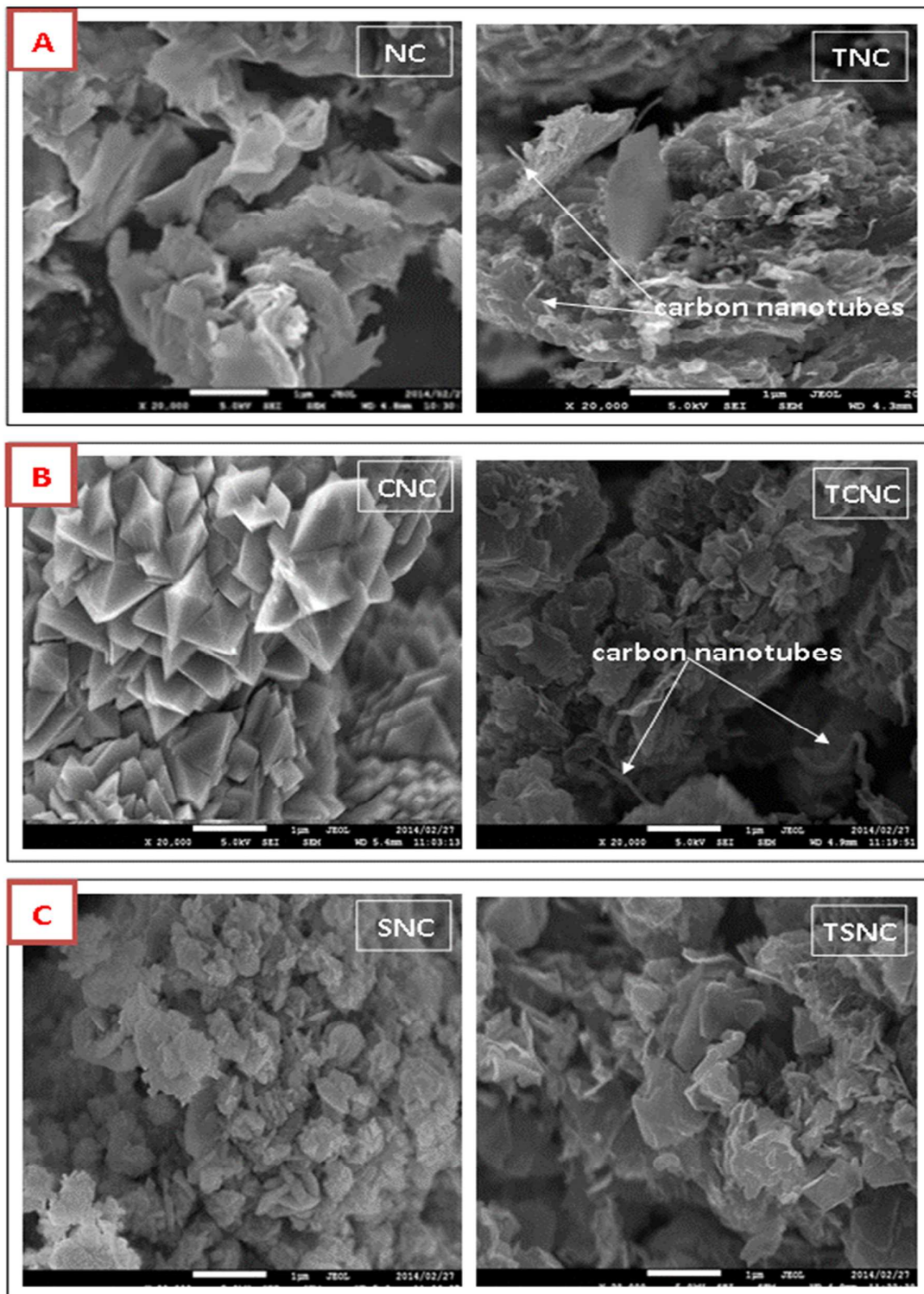


Figure 2: SEM images of A) Cloisite clay (NC), and its templated carbon (TNC); B) Zeolite synthesized from clear extract of cloisite clay (CNC), and its template carbon (TCNC); and C) Zeolite synthesized from slurry-form of cloisite clay (SNC), and its template carbon (TSNC).

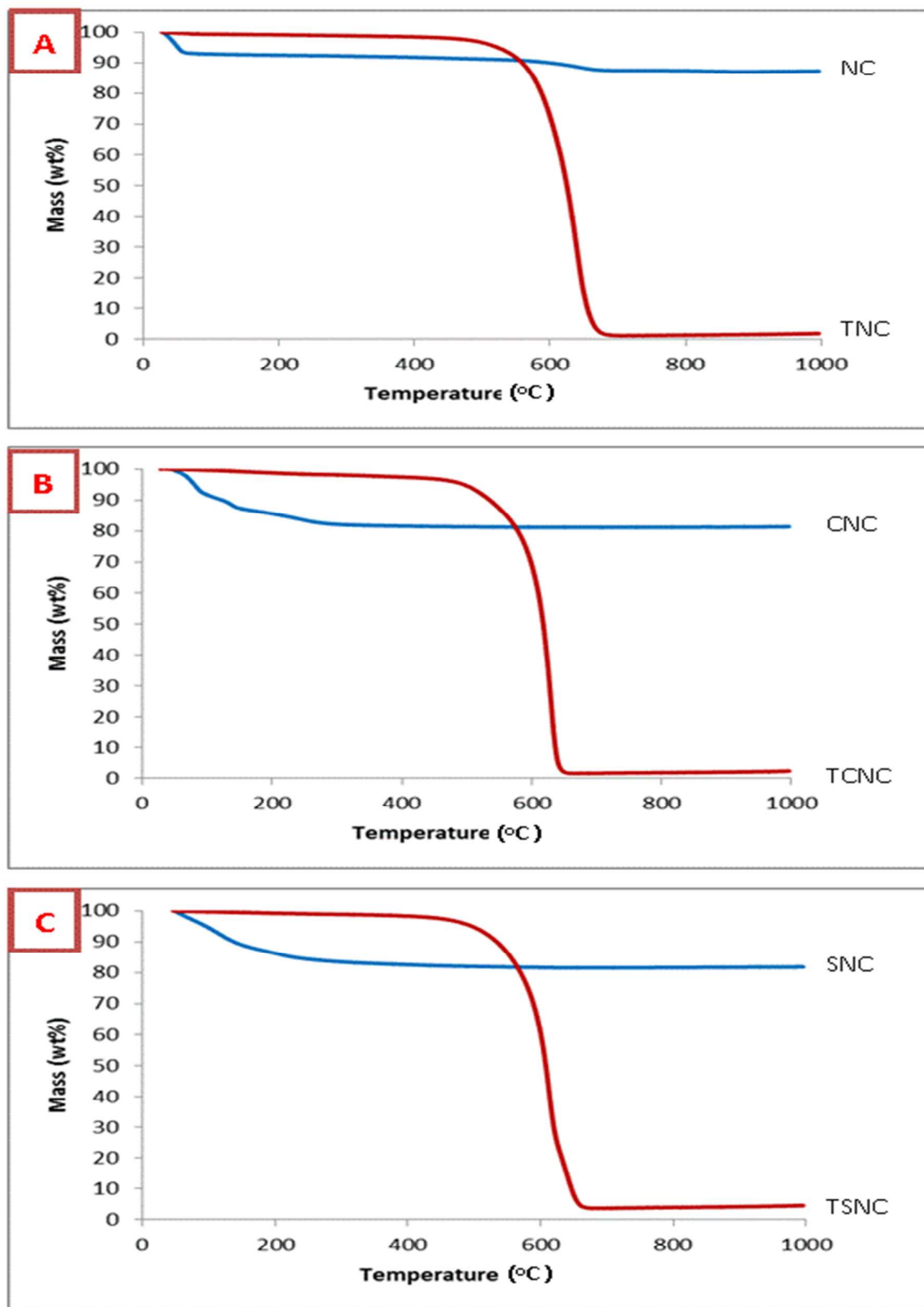


Figure 3: TGA plots of A) Cloisite clay (NC), and its templated carbon (TNC); B) Zeolite synthesized from clear extract of cloisite clay (CNC), and its template carbon (TCNC); and C) Zeolite synthesized from slurry-form of cloisite clay (SNC), and its template carbon (TSNC).

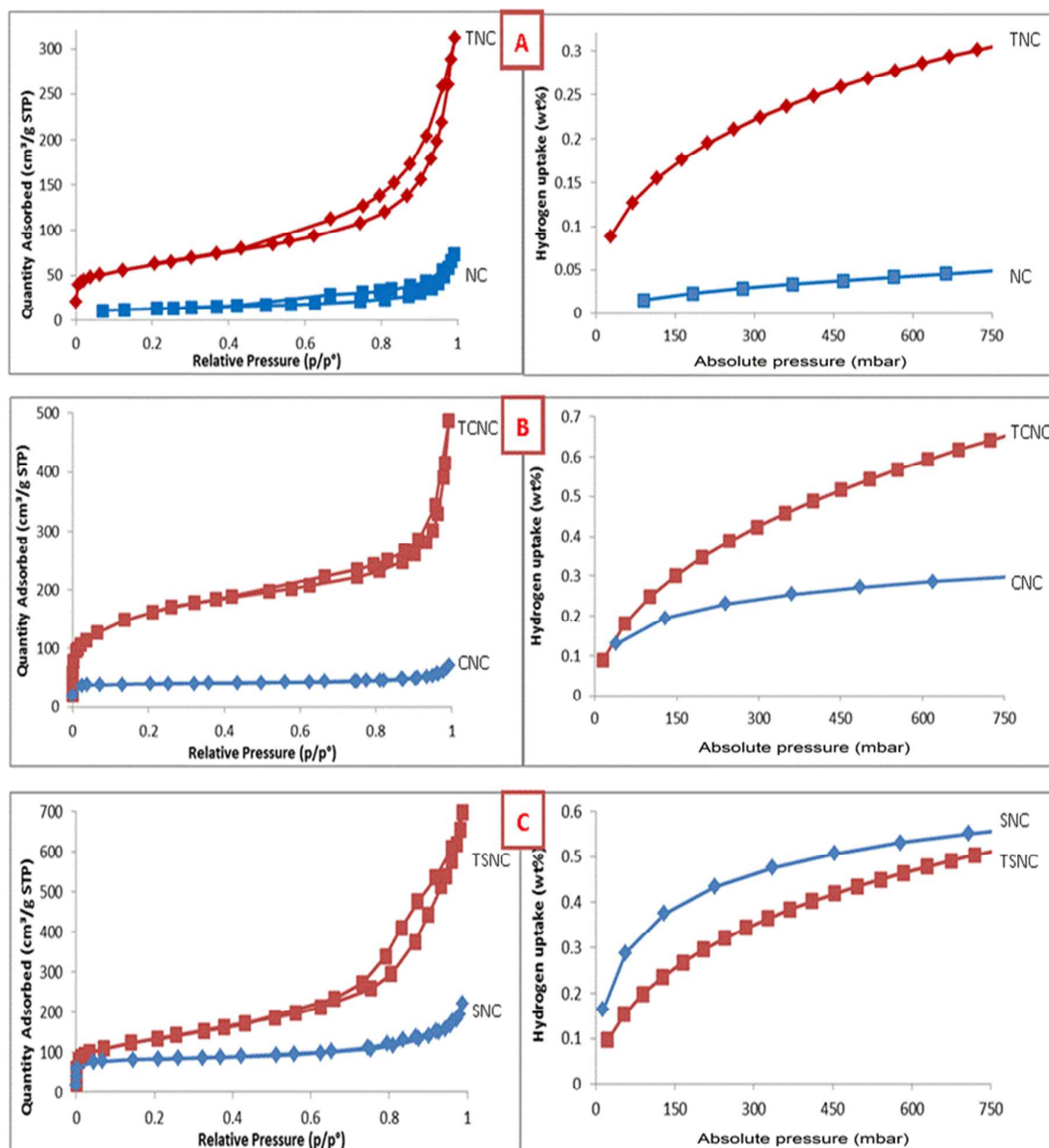


Figure 4: N₂-isotherm and hydrogen uptake plots of Cloisite clay (NC), and its templated carbon (TNC); B) Zeolite synthesized from clear extract of cloisite clay (CNC), and its template carbon (TCNC); and C) Zeolite synthesized from slurry-form of cloisite clay (SNC), and its template carbon (TSNC).

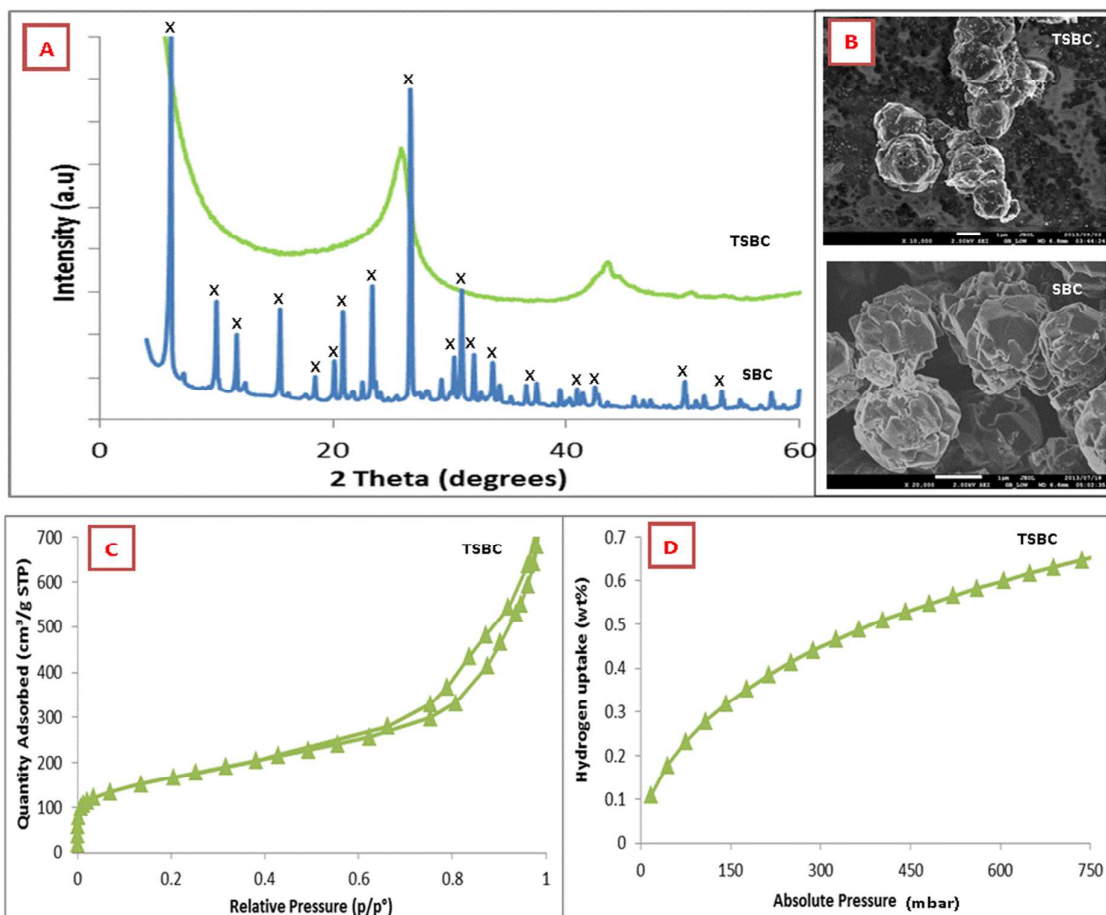


Figure 5: A) XRD patterns, B) SEM images of South African bentonite (SBC) and its template carbon (TSBC); C) N₂-isotherm and D) hydrogen uptake plots of template carbon from South African bentonite (TSBC).

Table 1: Surface areas and gravimetric hydrogen storage capacities of clay, clay-based zeolites and their respective template carbons.

Sample ID	Sample name	Surface area (m ² /g)	Gravimetric hydrogen storage capacity (wt%)
NC	Cloisite clay	45	0.1
TNC	Cloisite clay templated carbon	214	0.3
CNC	Cloisite clay-based zeolite (clear solution)	151	0.3
TCNC	Cloisite clay-based zeolite templated carbon (clear solution)	516	0.7
SNC	Cloisite clay-based zeolite (slurry solution)	317	0.6
TSNC	Cloisite clay-based zeolite templated carbon (clear solution)	461	0.5
TSBC	South African bentonite-based zeolite templated carbon (slurry solution)	569	0.7